An Initial Evaluation of Two Digital Airborne Imagers for Surveying Spruce Budworm Defoliation

F. J. Ahern
Canada Centre for Remote Sensing, Ottawa, Ontario K1A 0Y7, Canada
W. J. Bennett
INTERA Technologies Limited, Ottawa, Ontario K1S 5H4, Canada
E. G. Kettela
Maritime Forest Research Centre, Canadian Forestry Service, Fredericton, New Brunswick E3B 5P7, Canada

ABSTRACT: Insect damage is one of the most serious causes of forest depletion and growth loss in Canada. Informed forest management requires yearly information on insect damage in order to plan countermeasures and to revise predictions of future wood supply. Landsat MSS data have not generally been satisfactory for insect damage assessment. In 1983 the Canada Centre for Remote Sensing carried out an assessment of the ability of airborne multispectral scanners (mechanical and pushbroom) to detect current-year damage to softwood stands by spruce budworm larvae.

Data were acquired on 12 July 1983 with a mechanical scanner of approximately 25-m resolution and 16-km swath width and an electro-optical ("pushbroom") scanner of approximately 7-m resolution and 5-km swath width. Independent verification photography was acquired with a 240-mm mapping camera in the same aircraft with the multispectral scanners, and with 35-mm and 70-mm cameras in separate aircraft.

It was possible to detect and identify areas of spruce budworm defoliation very easily on natural color images made from the pushbroom scanner data, but similar images made from the lower resolution mechanical scanner data did not show areas of defoliation. Additional processing and the use of other bands of the mechanical scanner, including a band in the shortwave infrared (SWIR) region, were also unable to produce images showing areas of defoliation unambiguously. The primary reason for the different results was traced to the difference in spectral bands between the two sensors, with the improved radiometric resolution of the pushbroom scanner playing a contributing role. The difference in spatial resolution was not a significant factor.

Further work toward a system which could provide operational insect damage surveys is in progress at the Canada Centre for Remote Sensing.

INTRODUCTION

INSECTS AND DISEASE annually claim an estimated 88 million m³ of wood volume from Canadian forests (Baskerville, 1980). These timber losses affect the forestry sector at all levels, most notably at the resource management level. In eastern Canada, where forestry is fundamental to the economic health of the region, forest managers are battling one of the worst forest insect problems in Canada, the spruce budworm [*Choristoneura fumiferana* (Clem.)]. Periodic outbreaks of the budworm (three in the 20th century) have resulted in widespread defoliation, leading to growth loss (both radially and in height) and mortality of spruce-fir stands in Ontario, Quebec, and the Atlantic provinces. Timber reductions have been significant (Tables 1 and 2).

To monitor the activity of the spruce budworm and to plan and assess spray programs, federal and provincial forestry agencies conduct annual damage surveys. Aerial sketch mapping surveys* record the extent and severity of current-year defoliation, that is, damage to growth. The survey is carried out during a short period at the end of June and beginning of July, as soon as damage to current-year growth is complete. The damaged needles give the attacked trees the appearance of a reddish-brown sheath over the dark green older foliage. Light damage is often concentrated near the tops of the trees, while moderate and severe damage extend down the crown.

---

*Sketch mapping surveys are conducted by teams (a pilot and one or two mappers) in small aircraft. The teams fly along predetermined flight lines and sketch all areas of current damage in three categories onto a map: light (up to 30 percent defoliation), moderate (21 to 70 percent defoliation), and severe (over 70 percent defoliation).

Cumulative defoliation (damage done over several years) and mortality (dead and dying trees) are noted, but because they represent damage already done, they are not a primary focus of the annual survey.

Although conventional survey methods continue to supply foresters with useful information about the status of the spruce budworm, more reliable surveys related to individual stands could provide better timber forecasts (Erdle, 1985) when used as input to improved growth forecast models (McLean and Erdle, 1984).

This paper reports the results of a remote sensing project jointly undertaken by the Canada Centre for Remote Sensing (CCRS) and the New Brunswick Department of Natural Resources (NBDNR). The objective of the study was to carry out an initial evaluation of the potential of two digital airborne imagers, the MEIS-II pushbroom scanner (McColl et al., 1984) and a modified Daedalus 1260 (Zwich et al., 1980) for surveying spruce budworm defoliation.

Detecting current-year defoliation is a difficult remote sensing problem. Because it is only the remains of the damaged foliage that turn red-brown, defoliation is difficult to detect remotely. Secondly, the detectable red-brown stage of damage has a very short biowindow, lasting only two to three weeks. If during that period there is heavy rain or wind, the window is even shorter as damaged needles can be knocked off the trees. Finally, it is not easy to predict where an attack will occur, making project planning difficult. For these and other reasons related to data acquisition and resolution, Landsat MSS

data have not been useful for mapping current-year defoliation. Higher resolution airborne multispectral scanner data also proved to be ineffectual until Leckie and Gougeon (1981) were successful in digitally classifying four levels of cumulative defoliation (severe, moderate, light, healthy). Leckie and Ostaff report (in preparation) some success in using airborne multispectral scanner data to classify current-year defoliation into four levels in softwood stands but more difficulty in mixedwood stands. The CCRS-NBDNR study reported here was the first aimed at detecting spruce budworm damage by visual analysis of enhanced data.

STUDY AREAS

Two study sites were initially chosen, but marginal weather conditions, giving low-quality data, eliminated one of the sites. The remaining site is located north of Fredericton and extends for 25 km along the Miramichi River between Boiestown and Doaktown (NTS map sheet 21J) (Figure 1). The terrain is typically hilly and, in some places, relatively steep, except for the floodplain areas along the river. Forest cover in the area is mixed softwood-hardwood.

DATA ACQUISITION

As mentioned in the introduction, current-year spruce budworm damage is difficult to detect, and it is also difficult to predict where damage will occur. This fact complicates experimental planning. In addition, high spatial resolution is preferred, which reduces areal coverage and therefore reduces the probability that suitably damaged and undamaged (control) areas will be imaged. We attempted to cope with this problem by obtaining data over two test areas with a wide variety of sensors and scales (Table 3). The 29 June 1983 flight with the Canadian Forestry Service Cessna 170 provided an initial reconnaissance of the study areas and confirmed that the flight lines drawn up for the CCRS aircraft would cover both defoliated areas and areas lacking defoliation. This flight also aided the specification of flight

TABLE 1.   TIMBER LOSSES DUE TO SPRUCE BUDWORM IN THE LAST DECADE

Province	million m³	million ha
Newfoundland	38.4	*
Nova Scotia	30	*
New Brunswick	40	*
Quebec	*	8.7
Ontario	*	25
P.E.I.	*	*

*Data not available.
Source: Reed & Associates Ltd., 1980

TABLE 2.   1983 SPRUCE BUDWORM DEFOLIATION AND MORTALITY*

Province	Defoliation (1000 ha)	Mortality (1000 ha)
Newfoundland	67	458
Nova Scotia	358	800
P.E.I.	26	30
New Brunswick	2329	1000
Quebec	12266	11964
Ontario	9033	12119

*mortality = dead and dying trees
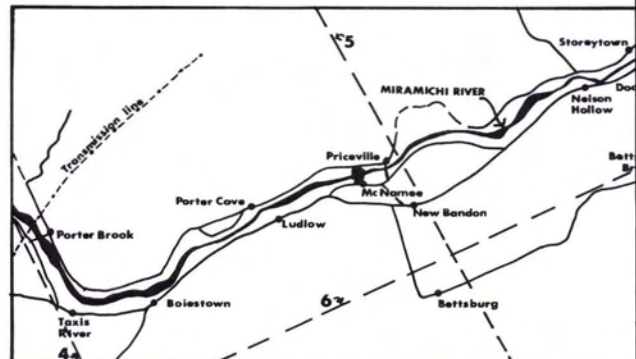Source: Kucera and Taylor, 1984

FIG. 1. Map of study area in central New Brunswick.

TABLE 3. AIRBORNE DATA CHARACTERISTICS

Sensor	Spectral Regions		Platform	Altitude (above ground)	Image Scale	Data Obtained
35-mm camera 50-mm lens	blue, green, red (natural color)		Cessna 170	900 m	various (oblique)	29 June 83
70-mm camera 80-mm lens	blue, green, red (natural color)		Cessna 172	1 200 m	1:15 000	10 July 83
RC-10 camera 150-mm lens	blue, green, red (natural color)		Falcon 50 (CCRS aircraft)	10 000 m	1:66 000	12 July 83
Daedalus 1260 multispectral scanner	3 4 5 7 8 9 10 11	450– 500 nm 500– 550 nm 550– 600 nm 630– 700 nm 680– 780 nm 770– 900 nm 870–1040 nm 1550–1750 nm	Falcon 50	10 000 m	25-m IFOV*	12 July 83
MEIS-II Pushbroom scanner	1 2 3 4 5	430– 460 nm 510– 540 nm 580– 610 nm 660– 690 nm 840– 900 nm	Falcon 50	10 000 m	7 m IFOV	12 July 83

*IFOV = Instantaneous field of view

lines for the 70-mm photography. The 70-mm and RC-10 photography was obtained to provide an independent record of defoliation for verification of the results obtained with the digital imagers.

The areas accessible by road and by foot along the transmission line cut (Figure 1) were visited to confirm the levels of defoliation damage which had been observed and photographed from the air. Close-up ground-based photography was also used to document the damage.

All defoliation levels were present in the study area: none to light in areas where the forest had been protected by aerial application of insecticide, and moderate to severe in populated areas and along water courses where spraying is not permitted. No backfeeding (destruction of previous years' foliage) was observed.

The visibility of the damage increased slightly between our initial reconnaissance flight on 29 June and approximately 5 July. From then on it remained essentially constant through the final data acquisition on 12 July, because there were no wind or rain storms to remove the damaged foliage from the trees.

Quantitative assessment of the degree of defoliation was not attempted because of the difficulty of obtaining adequate independent verification data; rather, this experiment was viewed as an initial evaluation of the MEIS-II and Daedalus 1260 scanners using enhanced images for qualitative visual assessment.

DATA ANALYSIS AND INTERPRETATION

MEIS DATA ANALYSIS

The MEIS data for flight lines 4 and 5 (see following section for a discussion of flight line 6) were copied from high-density tape to computer-compatible tape and then to disk. Visual inspection of the images and histograms showed that band 1 (430 to 460 nm) had very little contrast and a low signal-to-noise ratio, so this band was dropped from subsequent analysis.

The remaining four bands (corresponding to the green, yellow, red, and near infrared portions of the spectrum) were linearly contrast stretched and displayed on the Canada Centre for Remote Sensing Image Analysis System (CIAS) (Goodenough, 1979). Two radiometric artifacts were immediately apparent in color images formed from blue, green, and red displays of bands 2, 3, and 4 (Plate 1) and of bands 3, 4, and 5. First, a shift in hue towards the edges of the swath was noticed. This was expected as a result of a blue shift of approximately 30 nm in the central wave-length of the interference filters used to isolate the spectral bands of MEIS. Although there is a capability on the CIAS to measure and subtract systematic variation of radiance with view angle (program NEWSCN), we chose not to use this heuristic approach for fear of leaving in more subtle artifacts, which could be misleading in subsequent image interpretation.

The second radiometric artifact was colored ghost images of clouds. This problem was traced to a reflection of radiation from the interference filter of one band, to the aircraft window, and into the field of view of a second band. Steps have been taken to correct both radiometric problems.

Plate 1 is a natural color image made from the data of band 2 displayed as blue, band 3 displayed as green, and band 4 displayed as red. The data have been linearly contrast stretched before display.

If we ignore the edges of the image and areas of clouds, cloud shadows, and ghosts, it is possible to view this as a natural color image of a green forest with brown areas of discoloration. Transparencies made from the RC-10 negatives show brown discoloration in corresponding places, but they are difficult to see because the contrast-reducing effects of atmospheric path radiance and attenuation are not removed from the photography as they are from the digital MEIS data. The contrast of the RC-10 images is too low to reproduce the areas of defoliation in print. A comparison with the 70-mm photography shows that the areas of brown discoloration are indeed associated with spruce budworm defoliation (Plate 2).

MSS DATA ANALYSIS

Data from the Daedalus 1260 airborne multispectral scanner were also processed in an attempt to reveal spruce budworm defoliation. The Daedalus 1260 multispectral scanner obtains data over an angular range of $\pm 37.5°$ from nadir. Flight lines 4 and 5 were flown within 31 degrees of the solar azimuth. With this geometry, the radiance of a given ground-cover type will increase nearly symmetrically about nadir as a result of target bidirectional reflectance effects (Staenz et al., 1982) and variations in path radiance as a function of viewing angle (Turner et al., 1971). This resulting variation in radiance can be well fitted with a low order polynomial. Flight lines 4 and 5 were corrected for changes in radiance as a function of view angle with the program NEWSCN. Data from the individual bands were then contrast stretched to fill the available 0 to 255 range and a number of composite color images were formed (see Table 4). Principal component transformations were also performed on the data and color composite images were formed from the first three principal components.

None of these data treatments resulted in images that clearly showed spruce budworm defoliation distinctly from other sources of variation.

Flight line 6 was flown at approximately 90° to the solar azimuth to see whether data obtained with a scanner viewing the sun-lit forest obliquely (looking away from the sun) would be able to detect defoliation better than a nadir view. The water of the Miramichi River was used as a dark reference to measure and correct for the variation of path radiance with viewing direction. Subsequently, the program NEWSCN was used to correct for the average variation in the radiance of the forest as a function of view angle. Finally, the data were contrast stretched and made into color composites as for flight lines 4 and 5. The resulting images did not show spruce budworm defoliation any better than those formed from flight lines 4 and 5 data. Thus, this test was inconclusive and the airborne multispectral scanner was considered to have failed to detect spruce budworm defoliation.

In 1981, Leckie and Ostaff (in preparation) carried out a test of the CCRS Daedalus 1260 multispectral scanner for mapping current budworm defoliation in a somewhat more homogeneous spruce-fir forest approximately 110 km northwest of our study area. They were also unable to produce enhanced images which unambiguously showed current year defoliation. However, they did achieve moderate success using digital classification methods with a nine-band data set. It appears that their results are consistent with those reported here if one takes the differences in forest conditions and data analysis approaches into account.

MEIS-MSS COMPARISON

The MEIS and MSS data were processed further to determine what difference in charcteristics enables

TABLE 4.   AIRBORNE MSS IMAGES EXAMINED FOR SPRUCE BUDWORM DEFOLIATION

	DISPLAY COLOR		
	Blue	Green	Red
Contrast-stretched displays	3	7	10
of these airborne MSS	3	11	10
three-band combinations	7	5	10
	10	7	3
	11	10	3
	3	5	7
PRINCIPAL COMPONENTS ENHANCEMENTS			
Enhancement 1	PC1	PC2	PC3
Enhancement 2	Martin Taylor*		
	PC1 = brightness		
	PC2 = redness-greenness		
	PC3 = blueness-yellowness		
Enhancement 3	Reverse Martin Taylor		
	PC1 = brightness		
	PC2 = redness-yellowness		
	PC3 = blueness-greenness		

*The Martin Taylor enhancement is documented by Taylor (1973).

the MEIS data to show the defoliation when the MSS data could not.

Three MSS bands (4, 5, 7) corresponding as closely as possible to the MEIS bands 2, 3, and 4 were radiometrically matched to the MEIS data. This was done through a linear transformation, which matched the lower limit and mean value of the histogram of each MSS band to the lower limit and mean value of the corresponding MEIS band. The resulting image (Plate 3) still did not show brown discoloration corresponding to that visible in the MEIS image.

Next, to test whether the MEIS spatial resolution of 7 m compared to the MSS spatial resolution of 25 m played a significant role, the MEIS image was averaged with a sin x/x convolution with an effective size of 25 m between the innermost two zero crossings. This image is shown in Plate 4. The brown discoloration is *more* apparent in this image because of the reduction in radiometric variation brought about by spatial averaging. Because the defoliation areas are generally larger than 25 m, a spatial resolution of 25 m appears adequate to detect defoliation. The additional resolution of MEIS is not crucial.

Finally, random noise was added to the MEIS data to make MEIS match MSS in terms of noise variance. This was done by finding an area, in a cloud shadow, where the signal was low and essentially constant and the image variance was assumed to be representative of sensor noise. The variance of the data in each band of both sensors was measured. Then noise from a gaussian distribution was added to the 25-m resolution MEIS image to make its variance equal to that of the MSS image.

The additional noise made it more difficult to see the defoliated areas, but they are still visible in the degraded MEIS image and not in the MSS image. Thus, it seems that the better noise performance of MEIS relative to MSS explains part, but not all, of the success of MEIS.

Because the ability of MEIS to detect defoliation cannot be attributed entirely to its superior spatial or radiometric resolution compared to MSS, we turned our attention to the difference in spectral bands. Figure 2 shows two band intensities of five classes obtained from training areas in the MEIS image and Figure 3 shows two band intensities of the same five classes obtained from the same training areas in the MSS image. Water, mixedwood, and healthy conifer all have similar locations in both figures. With the MEIS bands (Figure 2) the hardwood class is lower in the red band, and overlaps with healthy conifer, and the defoliation class is separated from these, being brighter than both. In the MSS bands (Figure 3), the defoliation class overlaps the conifer and mixedwood classes, and the hardwood class is brighter than these. Figure 4 shows the spectral reflectance of the three main canopy components of defoliated balsam fir trees: healthy new needles, multi-year needles, and red material (consisting primarily of the remains of damaged needles). These
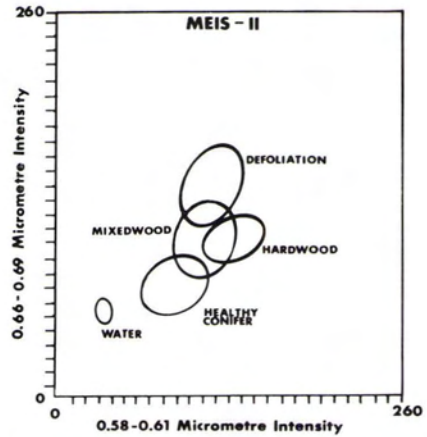

FIG. 2. Equi-probability ellipses of MEIS-II bands 3 and 4 for five classes.
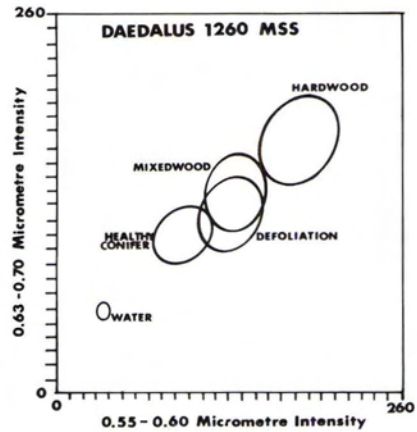

FIG. 3. Equi-probability ellipses of MSS bands 5 and 7 for the same five classes shown in Figure 4.
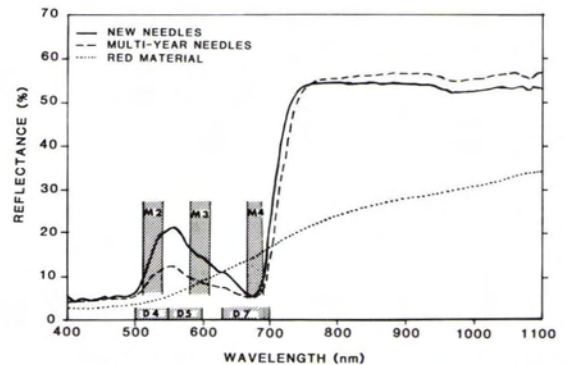

FIG. 4. Spectral reflectance curves of balsam fir foliage. Half-power points of Daedalus bands 4, 5, and 7 and MEIS-II bands 2, 3, and 4 are labelled D4, D5, D7 and M2, M3, and M4, respectively.

PLATE 1. Contrast-stretched natural color composite image formed from MEIS-II band 2 (0.51 to 0.54 micrometres) displayed as blue, band 3 (0.58 to 0.61 micrometres) displayed as green, and band 4 (0.66 to 0.69 micrometres) displayed as red. Resolution 7 m.

PLATE 2. 70-mm natural color photograph showing defoliation of individual trees in the area near New Bandon. The area photographed in Plate 2 is near the center of Plate 1, just south of the Miramichi River.

PLATE 3. Color composite image formed from Daedalus MSS band 4 (500 to 550 nm) displayed as blue, band 5 (550 to 600 nm) displayed as green, and band 7 (630 to 700 nm) displayed as red. These data have been radiometrically matched to the data displayed in Plate 1 as described in the text.

PLATE 4. MEIS-II data used for Plate 1 spatially averaged to 25-m resolution.

curves were obtained with a LICOR model LI-1800 spectrometer and integrating sphere in 1984 (Teillet et al., 1985). They show how the MEIS bands are narrower and better placed to distinguish between red material and multi-year needles, the principal canopy components which must be differentiated

to detect the presence or absence of current year spruce budworm defoliations. Note also that the 630 to 700 nanometre Daedalus band extends slightly into the infrared region where vegetation becomes highly reflective, especially if one remembers that the band edge is not sharp but extends beyond 700

nm into the infrared (see Zwick et al. (1980) for spectral response curves for the Daedalus MSS bands). The MEIS bandpasses are much more nearly rectangular. This probably explains why hardwoods are brighter than defoliated conifers in the Daedalus 630 to 700 nm band but darker than defoliated conifers in the MEIS-II 660 to 690 nanometre band. Thus, it is concluded that the major factor for the success of the MEIS sensor in detecting spruce budworm defoliation is its narrow, well-positioned spectral bands, particularly the red band.

RECOMMENDATION

The results presented in the above section show that the flexibility in selecting spectral bands and the high radiometric sensitivity of multi-element electro-optical imagers offer the opportunity to develop an airborne insect-damage mapping technology. Recent advances in growth-loss modelling (McLean and Erdle, 1984) combined with digital forest inventories (Erdle, 1985) mean that insect damage maps that are accurate at the stand level can be used for improved timber supply forecasting. Such forecasts can result in substantial improvements in actual timber supply through better harvest scheduling (Erdle, 1985).

An operational system capable of exploiting these results will require a high-altitude aircraft with a wide-swath pushbroom scanner and an inertial navigation system. The ground processing system must include an image analysis capability plus a geometric correction capability.

Additional research is necessary to ensure that these results can be consistently duplicated under the full range of atmospheric and environmental conditions likely to be encountered in operational use, and that a scanner with a wider field of view will detect defoliation levels under a wide range of illumination and viewing conditions. If this proves successful, work should begin on the definition of the components of the operational system.

CONCLUSIONS

In this study we have shown that it is possible to create natural color images showing moderate levels of current-year spruce budworm defoliation as a brown discoloration on a green forest background using data from an electro-optical pushbroom scanner. This demonstration suggests the possibility of a defoliation survey that would provide more accurate maps of current-year defoliation than those presently produced by aerial sketch mapping. This capability could improve spray program planning and effectiveness assessment, and ultimately improve the wood supply through better growth-loss predictions for harvest scheduling.

Successful detection of defoliation was achieved with the pushbroom (MEIS) scanner, but not with the mechanical (MSS) scanner. The mechanical scanner was unable to detect defoliation with both near-

nadir viewing, and when viewing the affected forest with a geometry that looked at the sun-lit sides of the trees.

The difference between the MEIS and MSS performance was traced primarily to a difference between the widths and placements of their spectral bands, particularly the red band. This diference was substantiated through subsequent ground-based spectroscopic studies (Teillet et al., 1985). The greater signal-to-noise ratio of MEIS compared to that of MSS was also shown to be important.

REFERENCES

Baskerville, G. L., 1980. Insects, Diseases and Forest Management: *Proceedings, Canadian Forest Congress, The Forest Imperative*, Toronto, Ontario, September 1980, pp. 52–54.

Erdle, T. A., 1985. *Harvest Scheduling and its Impact on Wood Supply* (Unpublished Report), New Brunswick Department of Natural Resources, Timber Management Branch, Fredericton, New Brunswick.

Goodenough, D. G., 1979. The Image Analysis System (CIAS) at the Canada Centre for Remote Sensing: *Canadian Journal of Remote Sensing*, Vol. 5, pp. 3–17.

Kucera, D. B., and R. G. Taylor, 1984. *Spruce Budworms Situation in North America 1983*, U.S. Department of Agriculture — Environment Canada Miscellaneous Publication Number 1441.

Leckie, D. G., and F. A. Gougeon, 1981. Assessment of Spruce Budworm Defoliation Using Digital Airborne MSS Data: *Proceedings, Seventh Canadian Symposium on Remote Sensing*, Winnipeg, Manitoba, September 1981, pp. 190–196.

Leckie, D. G., and D. P. Ostaff (In Preparation). Assessment of Current Defoliation Caused by the Spruce Budworm, Choristoneura Fumiferana (Clem) Using Airborne Multispectral Scanner Data.

McColl, W. D., R. A. Neville, and S. M. Till 1984. Multi-Detector Electro-Optical Imaging Scanner MEIS II: *Proceedings, Eighth Canadian Symposium on Remote Sensing and Fourth Conference of L'Association québécoise de télédétection*, Montreal, Quebec, May 1983, pp. 71–79.

McLean, D. A., and T. A. Erdle 1984. A Method to Determine Effects of Spruce Budworm on Stand Yield and Wood Supply Projections for New Brunswick: *The Forestry Chronicle*, June 1984, pp. 167–173.

Reed and Associated Ltd., 1980. Appendix IV, Recent Reductions in the Canadian Timber Base: *Proceedings, Canadian Forest Congress, The Forest Imperative*, Toronto, Ontario, September 1980, pp. 167–181.

Staenz, K., F. J. Ahern, and R. J. Brown 1981. The Influence of Illumination and Viewing Geometry on the

Reflectance Factor of Agricultural Targets: *Proceedings, Fifteenth International Symposium on Remote Sensing of Environment*, Environmental Research Institute of Michigan, Ann Arbor, Michigan, pp. 867–882.

Taylor, M. M., 1973. Principal Components Colour Display of ERTS Imagery, *Proceedings of the 3rd ERTS Symposium*, Volume 1, Section B, NASA, Washington, D.C., pp. 1877–1879.

Teillet, P. M., D. G. Leckie, D. Ostaff, G. Fedosejeus, and F. J. Ahern, 1985. Spectral Measurements of Tree Defoliation, *Proceedings of the 3rd International Colloquium on Spectral Signatures of Objects in Remote Sensing*, Les Arcs, France, pp. 511–516.

Turner, R. E., W. A. Malila, and R. F. Nalepka 1971. Importance of Atmospheric Scattering in Remote Sensing: *Proceedings, Seventh International Symposium on Remote Sensing of Environment*, Environmental Research Institute of Michigan, Ann Arbor, Michigan, pp. 1651–1697.

Zwick, H. H., W. D. McColl, and H. R. Edel, 1980. The CCRS DS1260 Airborne Multispectral Scanner (MSS), *Proceedings of the Sixth Canadian Symposium on Remote Sensing*, Canadian Aeronautics and Space Institute, pp. 643–648.

CALL FOR PAPERS

Intercommission Conference on
Fast Processing of Photogrammetric Data

Interlaken, Switzerland
2-4 June 1987

This joint conference of ISPRS Working Groups WG II/2 (Photogrammetric Digital Image Processing Systems), WG III/2 (On-Line Photogrammetric Triangulation), and WG V/6 (Digital and Real-Time Close-Range Photogrammetry) — organized by the International Society for Photogrammetry and Remote Sensing (ISPRS) and the Swiss Federal Institute of Technology Zürich (ETH) — intends to review the latest developments in algorithms, processing techniques, hardware, and software; to isolate the major problem areas; and to discuss the lines of research that need to be followed in the near future in order to further advance the technology. The topics to be addressed are defined by the terms of reference of the participating working groups as follows:

- Theoretical formulations, design, and performance of photogrammetric digital image processing systems.
- Formulation of estimation models, design of algorithms, and study of operational and software aspects for fast and reliable point positioning procedures.
- Hardware, computer algorithms, quality control, and software for real-time systems in machine vision, industrial process control, and change detection.

Those wishing to present a paper should submit an abstract by *15 January 1987* to

A. Gruen
Institute of Geodesy and Photogrammetry
ETH Honggerberg
CH-8093 Zürich
Switzerland